HIGH-TEMPERATURE DIRECT VAPOR GENERATION ORGANIC RANKINE CYCLE IN THE CONCENTRATED SOLAR POWER APPLICATION

Pengcheng Li[1, 3], Jing Li[2,*]
[1]Hefei University of Technology, School of Automobile and Traffic Engineering, Hefei, Anhui Province, China
[2]University of Hull, Cottingham Rd, Hull, HU6 7RX, United Kingdom
[3]Dongfang Boiler Group Co., Ltd., Zigong, Sichuan Province, China

E-mail: Jing.Li@Hull.ac.uk

ABSTRACT

A novel direct vapor generation solar thermal power system in the high-temperature application (>350°C) is proposed. The system mainly consists of a solar field, two-tank thermal storage, and cascade organic/steam Rankine cycle (ORC-SRC). Compared with the commercial concentrated solar power (CSP) plants using synthetic oil for heat carrier purpose only, the novel system employs the oil for heat collection, thermal storage and power conversion. The thermal oil is vaporized directly in the solar field. The outlet fluid can be either in liquid, binary phase, or vapor state, depending on the solar radiation. Vapor in the high-temperature tank flows into the ORC turbine and expands. The exhaust vapor is condensed, and the heat is released to the bottom SRC. The system tackles the challenges in the direct vapor generation technology: stable power conversion under fluctuating solar radiation and long-term reliable storage. The fundamentals of the system are illustrated. Mathematical models are built. Simulation is conducted by using Therminol® VP-1 as the fluid. The results indicate that the proposed system significantly increases the average temperature of the solar field owing to the fluid vaporization. Compared with a conventional CSP system using two-tank thermal storage, the proposed system has a higher power efficiency (42.01% vs. 37.93%). By optimizing the steam evaporation temperature of the bottom SRC, a further efficiency increment is expected with a large storage capacity. The direct vapor generation solar field of thermal oil can also be combined with a molten salt unit. Though two-tank oil storage is exemplified in the simulation, the increased efficiency and enlarged storage capacity are achievable when two-tank molten salt storage is employed.

1 INTRODUCTION

Thermal power generation is an important application of solar energy. Unlike solar PV technologies, the power generation from solar thermal storage plants is dispatchable and self-sustainable. Up to now, state-of-the-art commercial and demonstration CSP plants use synthetic oil as heat carrier in the collectors (Concentrating Solar Power Projects by Technology-NREL, 2021). The technical feasibility has been well demonstrated. Therminol® VP-1 is a typical synthetic oil composed of 73.5% diphenyl oxide and 26.5% biphenyl. It possesses exceptional thermal stability and low viscosity in a wide temperature range up to 400 °C. It can be used as a liquid heat transfer fluid or as a boiling-condensing heat transfer medium up to its maximum temperature. Its potential in high-temperature ORCs has been investigated in the literature (Vescovo, 2019). However, at present the biphenyl/diphenyl oxide mixture has not been chosen as the power cycle fluid of a CSP system.

Some organic fluids have been investigated for direct vapor generation (DVG) in the solar field (Casati *et al*., 2013; Li *et al*., 2016). Replacing water with the organic fluids, secondary heat transfer can be avoided and the technical challenges of wet steam turbines are overcome in the DVG systems. Notably, the organic fluids of the DVG system in the literature work at a temperature lower than 300°C, and are mainly siloxanes and refrigerants. The biphenyl/diphenyl oxide mixture has not been discussed in the DVG application.

If the mixture is in place of water for direct vapor generation and power conversion, it may face some challenges similar to those of direct steam generation solar power systems, including lacks of reliable control strategy under fluctuating solar radiation and long-term cost-effective storage. As the oil is not only the storage medium but also the power cycle fluid, its temperature decrement during discharge leads to off-design operation of the power cycle. The turbine intake pressure decreases almost exponentially with the temperature decrement. The available temperature drop will be limited to avoid inefficient power conversion (Li *et al*., 2019), resulting in a small and uneconomical storage capacity.

To tackle these challenges, a novel CSP system using cascade organic/steam Rankine cycle (ORC-SRC) is proposed. It is the first time that the cascade ORC-SRC has been combined with dual tanks in the CSP application. Stable power conversion is guaranteed under fluctuating solar radiation, with a remarkably enlarged storage capacity. The biphenyl/diphenyl oxide mixture is adopted as the heat transfer, storage and ORC fluid. Vapor is directly generated in the solar field. The collectors benefit from the constant temperature and efficient heat transfer in the binary phase region. The average temperature of the collectors is elevated. Meanwhile, the thermal efficiency is appreciably higher than the conventional indirect systems thanks to the cascade cycle.

2 SYSTEM DESCRIPTION

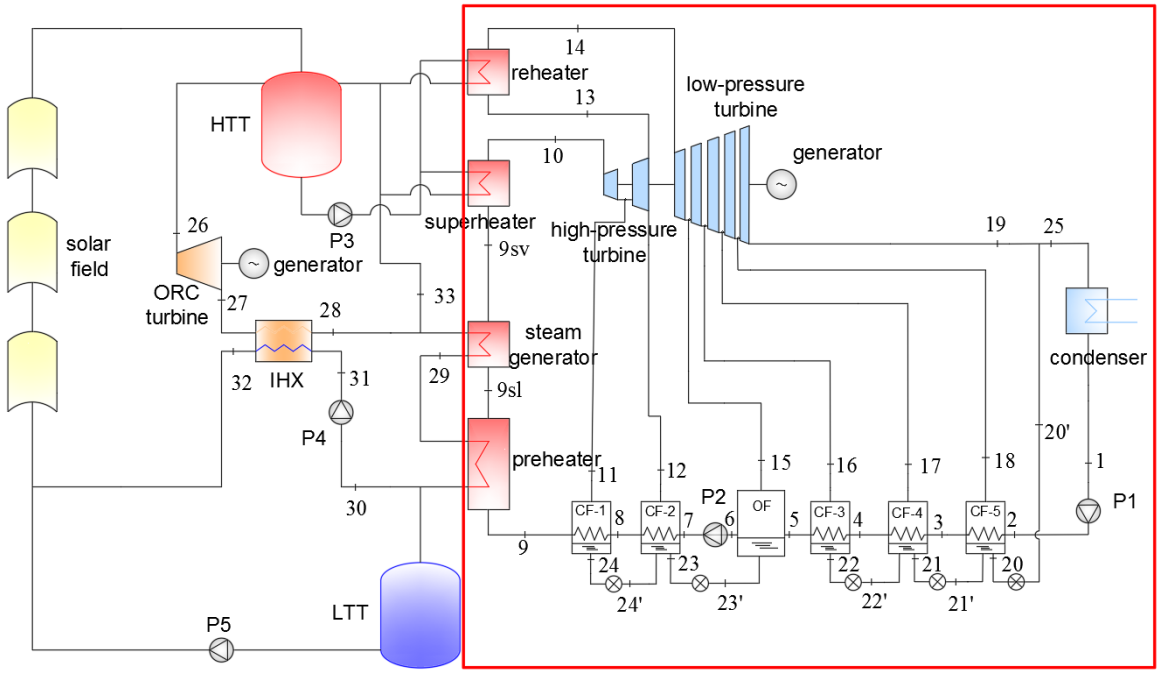

Figure 1: Schematic diagram of the solar ORC-SRC system

Fig. 1 shows the schematic diagram of the proposed DVG system using two-stage tanks and ORC-SRC. The system is composed of the solar field, high-temperature tank (HTT), low-temperature tank (LTT), and ORC-SRC unit. Therminol® VP-1 in HTT is in the vapour-liquid binary state. The right part in the red box represents the conventional regenerative SRC. Two extractions, 11 and 12, are taken from the high-pressure turbine to the closed feedwaters (CF-1, CF-2). Four extractions, 15-18, are bled to the closed feedwaters (CF-3, CF-4, CF-5) and a deaerator (open feedwater, OF) from the low-pressure turbine. The closed feedwater heaters are shell-and-tube-type recuperators, which are used to increase the feedwater temperature through condensation of the extracted steam. The deaerator is a direct contact-type heat exchanger in which streams at different temperatures are mixed to form a stream at an intermediate temperature at saturated liquid conditions (Padilla *et al*., 2011). The *T-s* diagram of the cascade ORC-SRC is graphed in Fig. 2.

The system can operate in many modes, depending on the solar radiation and the HTT temperature. Two main modes are introduced as follows.

Mode 1: Simultaneous heat collection and ORC-SRC power conversion, as marked in red lines in Fig. 3 (a). It is assumed that when the direct normal irradiance (I_{DN}) in the design condition is 400 W/m^2, the solar heat gain is equal to the rated heat input of the ORC-SRC. The system operates in this mode when I_{DN} ≥400 W/m^2. Therminol® VP-1 leaving LTT is heated and vaporized in the solar field. The outlet fluid can be either in liquid, binary phase or vapor state. Technically, binary phase state is preferable to prevent overheat of the oil. The vapour at the top HTT drives the ORC turbine, while the liquid in the HTT superheats and reheats the steam entering the high-pressure and low-pressure steam turbines. The mass flow rate of the oil through P5 varies with the radiation to store the residual solar heat in the HTT. The system may also operate in this mode when the solar radiation is lower than 400 W/m^2 (e.g., transient period with passing clouds) for which the ORC-SRC is at part-load operation and the HTT temperature is slightly lower than the nominal value.

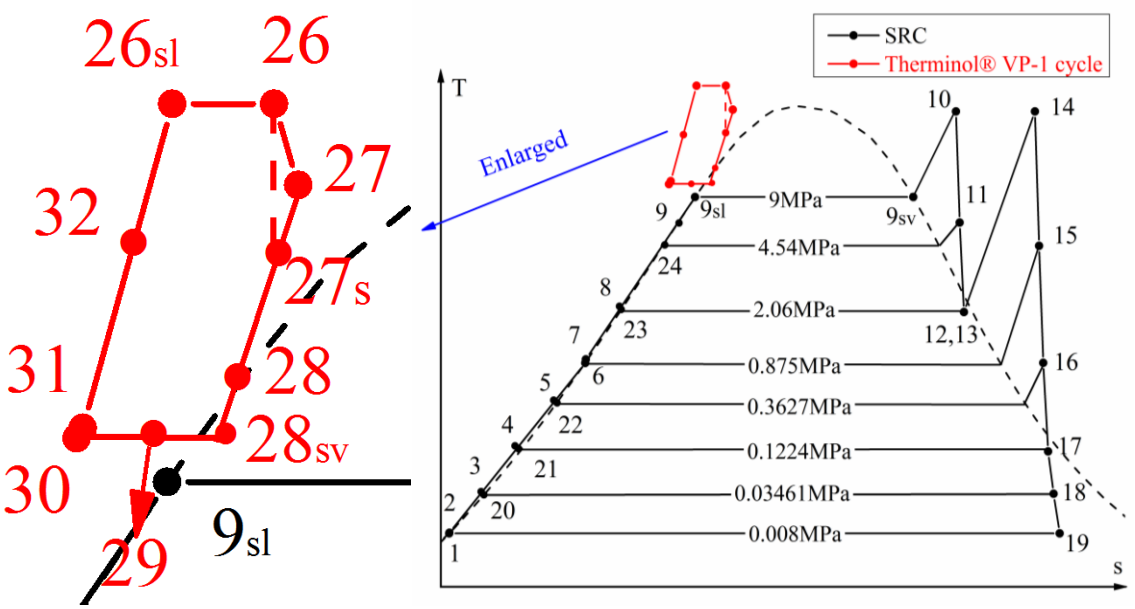

(a) Enlarged top ORC (b) Cascade ORC-SRC

Figure 2: *T-s* diagram of the cascade ORC-SRC

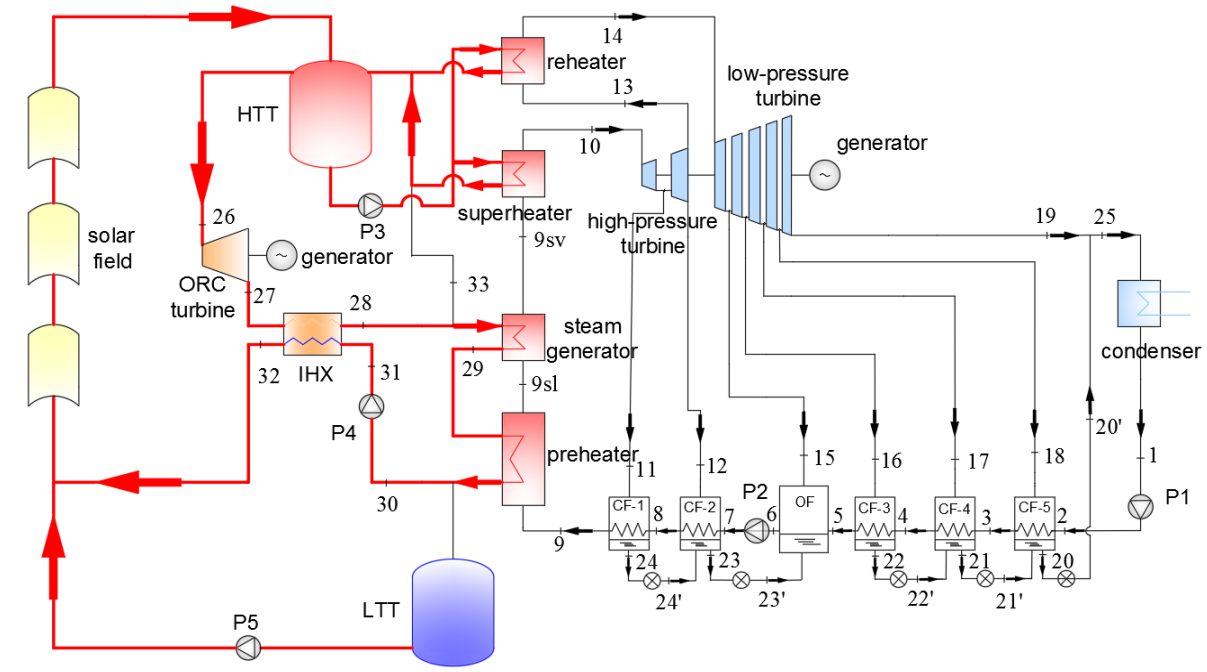

(a) Rated mode

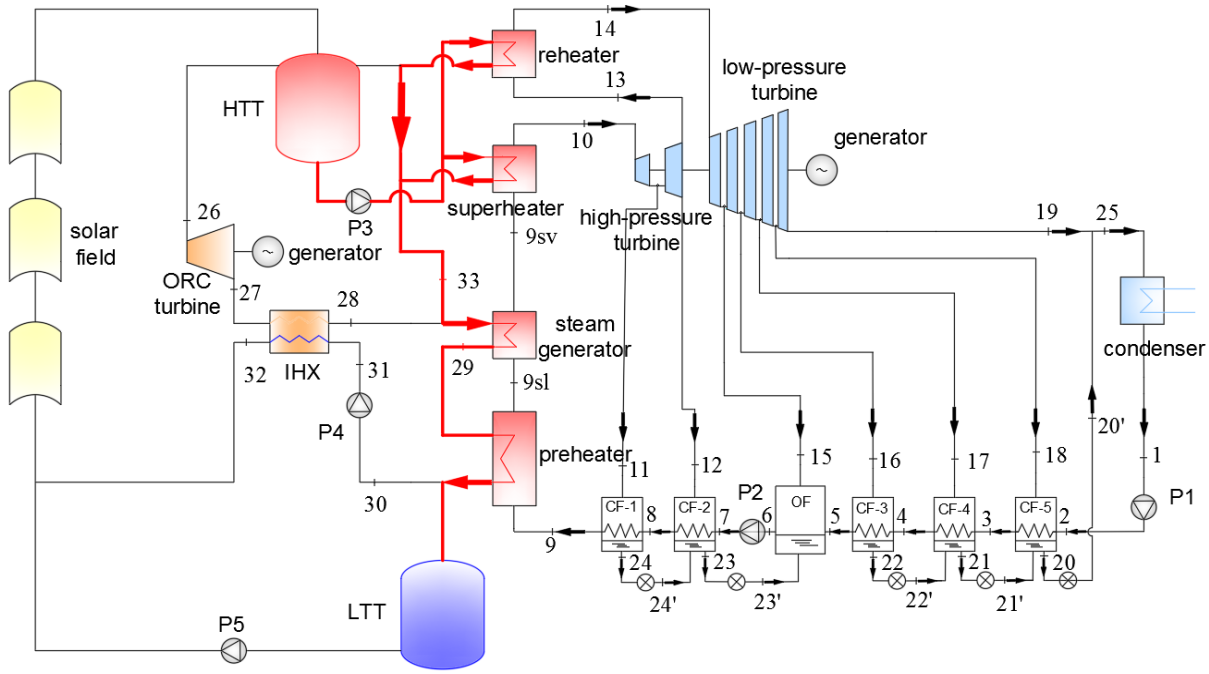

(b) Heat discharge mode

Figure 3: Different operating modes

Mode 2: Heat discharge mode. There can be two-step heat discharge. In the first step, the vapor generated by flashing in HTT drives the ORC-SRC. As the temperature drop of HTT in this step is limited, most heat will be released via the second step heat discharge, as presented in Fig. 3 (b). The discharge process is the same as that of a conventional dual-tank based indirect CSP system: Therminol® VP-1 in the HTT flows into the LTT and the released heat is used only to drive the SRC.

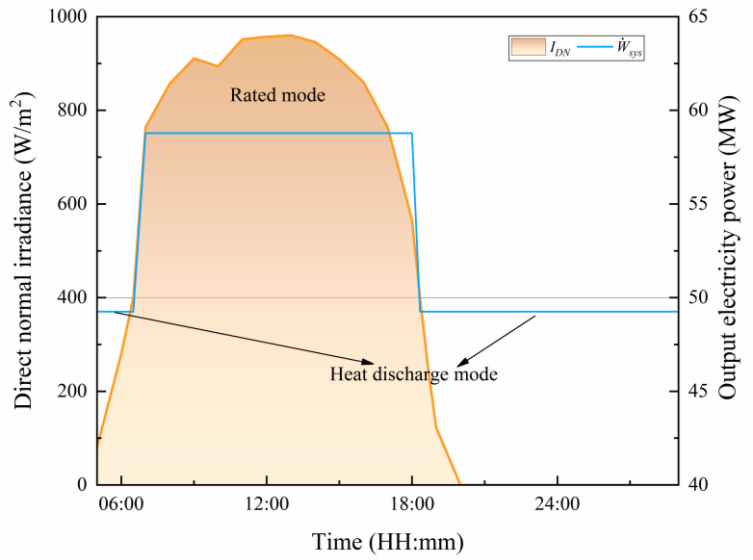

Figure 4: Variations of the direct normal irradiance and the operation modes throughout the day

A possible variation of the total power output throughout a day is shown in Fig.4. As is well-known, I_{DN} is subject to the location as well as time and season. In the paper, the reference I_{DN} of 400 W/m^2 is only used to illustrate the operating modes of the proposed system. This value can vary (e.g., 450 or 500 W/m^2) for practical design, depending on the size of the solar field and local meteorological conditions. Therefore, the reference I_{DN} in Fig. 4 will not affect the results as this paper focuses on the performance of the ORC-SRC.

The proposed system has several distinct advantages. First, it will have a higher efficiency than a conventional SRC, as the latter is just a subcycle of the ORC-SRC. Second, a more significant temperature drop from the HTT to the LTT may be available. In a conventional dual-tank CSP system, the HTT and LTT temperatures are around 390 and 300 °C. The water evaporation temperature is about 310 °C for the sake of efficient power conversion. Most heat is input in the evaporation process due to the large latent heat of water. The LTT temperature is relatively high to avoid an uneconomically low efficiency. The ORC-SRC can offer lower LTT temperature and water evaporation temperature, which leads to a decreased SRC efficiency but possibly an increased overall cycle efficiency. Therefore, a lower LTT temperature and larger storage capacity are achievable with a higher ORC-SRC efficiency. Third, efficient heat collection is facilitated with low technical requirement, due to the high evaporation temperature and low saturation pressure of Therminol® VP-1. For instance, the saturation pressure is merely 0.959 MPa at 390 °C (Eastman Corp, 2021), while the saturation pressure of water is 4 MPa at 250 °C. The pressure bearing problems in both the tanks and the absorber tubes in conventional direct steam generation systems are greatly alleviated. The life expectancy of the tubes will be longer and the investment of the tanks will be smaller.

3 MATHEMATICAL MODELS

3.1 Heat Exchangers

The heat balance in the preheater, steam generator and internal heat exchanger (IHX) is defined as

$$m_{VP-1}(h_{29} - h_{30}) = m_{steam}(h_{9sl} - h_9) \quad (1)$$

$$m_{VP-1}(h_{28} - h_{29}) = m_{steam}(h_{9sv} - h_{9sl}) \quad (2)$$

$$h_{27} - h_{28} = h_{32} - h_{31} \quad (3)$$

The pinch point that the minimum temperature difference (ΔT_{min}) occurs is at the outlet of saturated water for the preheater

$$T_{30} - T_{9sl} = T_{28sv} - T_{9sl} = \Delta T_{min} \quad (4)$$

The IHX efficiency is calculated by.

$$\varepsilon_{IHX} = \frac{h_{27}-h_{28}}{h_{27}-h(T_{31},p_{28})} \quad (5)$$

where $h(T_{31}, p_{28})$ is the specific enthalpy of the working fluid at the pump's outlet temperature of T_{31} and the condensing pressure of p_{28}. This would be the theoretical lowest enthalpy to which the hot stream could be condensed. $h(T_{31}, p_{28})$ is close to h_{28sv} due to a limited liquid temperature increment after pressurization.

The terminal temperature difference, which is the difference between the saturation temperature of the extraction steam and the feedwater outlet temperature, is set at 1.5 °C (Mohammadi *et al*., 2018).

$$T_{sv@p11} - T_9 = T_{sv@p12} - T_8 = T_{sv@p15} - T_6 = T_{sv@p16} - T_5 = T_{sv@p17} - T_4 = T_{sv@p18} - T_3 = 1.5 \quad (6)$$

The drain cooler approach, which is the difference between the drain outlet temperature and the feedwater inlet temperature, is set at 5 °C (Mohammadi *et al*., 2018).

$$T_{24} - T_8 = T_{23} - T_7 = T_{22} - T_4 = T_{21} - T_3 = T_{20} - T_2 = 5 \quad (7)$$

The heat balance in CF-1 and CF-2 is defined as

$$m_{11}(h_{11} - h_{24}) = m_{steam}(h_9 - h_8) \quad (8)$$

$$m_{12}h_{12} + m_{24}h_{24,} + m_7h_7 = m_8h_8 + m_{23}h_{23} \quad (9)$$

The same is true for OF, CF3, CF4 and CF-5. Besides, the enthalpy remains the same after throttling. $h_{24,}=h_{24}$, $h_{23,}=h_{23}$, $h_{22,}=h_{22}$ and $h_{21,}=h_{21}$.

3.2 Expanders

The work produced by the high-pressure and low-pressure turbines is determined by

$$W_{HT} = m_{steam}h_{10} - m_{11}h_{11} - m_{12}h_{12} - m_{13}h_{13} \quad (10)$$

$$W_{LT} = m_{14}h_{14} - m_{15}h_{15} - m_{16}h_{16} - m_{17}h_{17} - m_{18}h_{18} - m_{19}h_{19} \quad (11)$$

where ε_{HT} and ε_{LT} are the efficiencies of high-pressure and low-pressure turbines, respectively.

$$\varepsilon_{HT} = \frac{h_{10}-h_{11}}{h_{10}-h_{11s}} = \frac{h_{11}-h_{12}}{h_{11}-h_{12s}} \quad (12)$$

$$\varepsilon_{LT} = \frac{h_{14}-h_{15}}{h_{14}-h_{15s}} = \frac{h_{15}-h_{16}}{h_{15}-h_{16s}} = \frac{h_{16}-h_{17}}{h_{16}-h_{17s}} = \frac{h_{17}-h_{18}}{h_{17}-h_{18s}} = \frac{h_{18}-h_{19}}{h_{18}-h_{19s}} \quad (13)$$

For the ORC turbine

$$W_{OT} = m_{VP-1}(h_{26} - h_{27}) = m_{VP-1}(h_{26} - h_{27s})\varepsilon_{OT} \quad (14)$$

where ε_{OT} denotes the ORC turbine efficiency.

3.3 Pumps

The work consumed by P1, P2 and P4 is calculated by

$$W_{P1} = m_1(h_2 - h_1) = m_1(h_{2s} - h_1)/\varepsilon_P \quad (15)$$

$$W_{P2} = m_{steam}(h_7 - h_6) = m_{steam}(h_{7s} - h_6)/\varepsilon_P \quad (16)$$

$$W_{P4} = m_{VP-1}(h_{31} - h_{30}) = m_{VP-1}(h_{31s} - h_{30})/\varepsilon_P \quad (17)$$

where ε_P is the pump efficiency.

3.4 Entropy of Therminol® VP-1 at saturated state

The thermophysical properties of Therminol® VP-1 can not be acquired from REFPROP, but its saturation state parameters at intervals of 10 °C can be obtained from a supplier (Eastman Corp, 2021).

The parameters of saturated state at any temperature (like T, p, h, v) can be calculated by linear interpolation.
The entropy of saturated state at different temperatures can be derived from thermodynamic relation.

$$dh = Tds + vdp \tag{18}$$

In the simulation, s_{30} ($s_{313.34°C,sl}$)is the reference state and s_{30} =3 kJ/kg • K. $s_{320°C,sl}$ can be deduced by integrating Eq. (18). $\int_{313.34°C,sl}^{320°C,sl} dh = \int_{313.34°C,sl}^{320°C,sl} Tds + \int_{313.34°C,sl}^{320°C,sl} v_{sl}dp$. Saturated liquid enthalpy at T_{30} ($h_{313.34\,°C,sl}$) can be calculated by linear interpolation. T in each integral interval can be replaced by the average of the initial and final temperatures, the same is true for v_{sl}. Similarly, $s_{330°C,sl}\cdots, s_{390°C,sl}$ are acquired and $s_{390°C,sl} = s_{26\mathrm{sl}}$ =3.303 kJ/kg • K. As $dp = 0$ in the binary phase region, $\int_{26_{\mathrm{sl}}}^{26} vdp = 0$ and $\int_{390°C,sl}^{390°C,sv} dh = \int_{390°C,sl}^{390°C,sv} Tds$, $s_{390°C,sv}$ can thus be derived and $s_{390°C,sv} = s_{26}$ =3.624 kJ/kg • K. Analogously, $s_{313.34°C,sv} = s_{28sv}$ =3.4498 kJ/kg·K.

3.5 The outlet enthalpies of ORC turbine and IHX

The superheated state enthalpy at the outlet of ORC turbine (h_{27}) cannot be derived directly. Previously, the authors have developed an ORC efficiency model based on the equivalent hot side temperature (T_{EHST}) (Li *et al*., 2016), in which only the saturation parameters are required.

$$T_{EHST} \approx \frac{h_{26}-h_{30}-v_{30}(p_{26}-p_{30})}{s_{26}-s_{30}} \tag{19}$$

The efficiency of ORC with the most basic structure ($\eta_{ORC,b}$) can be built with the assistance of T_{EHST}. $\eta_{ORC,b}$ is in good agreement with the actual. The relative error is from -0.7% to 3.4% on the use of 27 fluids (Li *et al*., 2016).

$$\eta_{ORC,b} = \left(1-\frac{T_{30}}{T_{EHST}}\right)\cdot\frac{\varepsilon_{OT}\cdot\varepsilon_g+v_{30}(p_{26}-p_{30})/\left(\varepsilon_P\cdot\int_{26}^{28sv} v_{sv}dp\right)}{1+v_{30}(p_{26}-p_{30})/\left(\int_{26}^{28sv} v_{sv}dp\right)} \tag{20}$$

where $\int_{26}^{28sv} v_{sv}dp$ can be obtained by piecewise integration and then summation. It can be inferred from Table 1 that $T_{26} = T_{HTT}$ =390 °C and T_{28sv} =10+T_{9sl}=313.34 °C

$$\int_{26}^{28sv} v_{sv}dp = \int_{390}^{380} v_{sv}dp + \int_{380}^{370} v_{sv}dp + \cdots + \int_{330}^{320} v_{sv}dp + \int_{320}^{313.34} v_{sv}dp \tag{21}$$

Meanwhile, $\eta_{ORC,b}$ can be expressed as

$$\eta_{ORC,b} = \frac{(h_{26}-h_{27})\cdot\varepsilon_g-(h_{31}-h_{30})}{h_{26}-h_{31}} \tag{22}$$

h_{27} can be then deduced. Most ORC fluids at liquid state are not compressible, and most of the heat is taken out by the condensation process (Li *et al*., 2016). Therefore,

$$h_{31s} \approx h_{30} + v_{30}(p_{31s} - p_{30}) \tag{23}$$

where $p_{31s} = p_{31} = p_{32} = p_{26}$ =0.959 MPa. p_{30}, h_{30} and v_{30} can be obtained by linear interpolation. h_{27} can be deduced by combining Eqs. (17) and (19-23) as the ideal power output is determined by the heat input and ORC efficiency.
Given $h(T_{31}, p_{28})$ and ε_{IHX}, h_{28} can be obtained from Eq. (5). The outlet temperature of P4 (T_{31}) cannot be deduced as it is subcooled state. Notably, the temperature rise of ORC fluid is generally less than 1 °C after pressurization. As $T_{30} = T_{28sv}$ and $p_{28sv} = p_{28}$, the temperature corresponding to $h(T_{31}, p_{28})$is approximately 1 °C higher than that of h_{28sv}. $h(T_{31}, p_{28})$ can be regarded as saturated vapor enthalpy at T_{31}. h_{32} can be calculated according to Eq. (3).
With the heat recovered ($h_{32} - h_{31}$) from the IHX and the power output of a basic ORC, the efficiency of the ORC with the IHX can be deduced as follows.

3.6 Thermal efficiency

The thermal efficiency of the ORC with Therminol® VP-1 is defined by

$$\eta_{ORC} = \frac{W_{ORC}}{m_{VP-1}(h_{26}-h_{32})} = \frac{(h_{26}-h_{27})\cdot\varepsilon_g-(h_{31}-h_{30})}{h_{26}-h_{32}} \quad (24)$$

The bottom SRC represents the conventional two-tank system, and its thermal efficiency is expressed by

$$\eta_{SRC} = \frac{W_{SRC}}{m_{steam}(h_{10}-h_9)+m_{13}(h_{14}-h_{13})} = \frac{(W_{HT}+W_{LT})\cdot\varepsilon_g-W_{P1}-W_{P2}}{m_{steam}(h_{10}-h_9)+m_{13}(h_{14}-h_{13})} \quad (25)$$

The heat to power conversion efficiency of the cascade ORC-SRC is

$$\eta_{ORC-SRC} = \frac{W_{SRC}+W_{ORC}}{m_{steam}(h_{10}-h_{9sv})+m_{13}(h_{14}-h_{13})+m_{VP-1}(h_{26}-h_{32})} \quad (26)$$

In this simulation, some assumptions are made as listed in Table 1. Besides, the power consumption of the cooling tower is not considered. As the proposed system is innovative, this paper focuses on its principles, advantages, and differences from a conventional indirect CSP using thermal oil. The cooling unit (either wet or dry cooling) is similar to that of a conventional CSP and therefore is not the focus.

Table 1: Specific parameters for calculation.

Term	Value
Gross electric power of SRC (Padilla *et al.*, 2011), $(\boldsymbol{W_{HT}+W_{LT}})\cdot\boldsymbol{\varepsilon_g}$	50 MW
High-pressure turbine efficiency (Montes *et al.*, 2009, Padilla *et al.*, 2011), $\boldsymbol{\varepsilon_{HT}}$	0.855
Low-pressure turbine efficiency (Montes *et al*., 2009, Padilla *et al.*, 2011), $\boldsymbol{\varepsilon_{LT}}$	0.895
High pressure (Montes *et a*l., 2009, Padilla *et a*l., 2011), $\boldsymbol{p_1}$	9 MPa
Pressure of extraction no. 1 (Montes *et al*., 2009), $\boldsymbol{p_{11}}$	4.54 MPa
Pressure of extraction no. 2 (Montes *et al*., 2009), $\boldsymbol{p_{12}}$	2.06 MPa
Pressure of extraction no. 3 (Montes *et al*., 2009), $\boldsymbol{p_{15}}$	0.875 MPa
Pressure of extraction no. 4 (Montes *et al*., 2009), $\boldsymbol{p_{16}}$	0.3627 MPa
Pressure of extraction no. 5 (Montes *et al*., 2009), $\boldsymbol{p_{17}}$	0.1224 MPa
Pressure of extraction no. 6 (Montes *et al*., 2009), $\boldsymbol{p_{18}}$	0.03461 MPa
Steam condensation pressure (Montes *et al*., 2009, Padilla *et al*., 2011), $\boldsymbol{p_{19}}$	0.008 MPa
Pressure drop in feed water extractions lines (Mohammadi *et al*., 2018)	3%
High-pressure turbine inlet temperature (Montes *et al*., 2009), $\boldsymbol{T_{10}}$	370 °C
HTT temperature (Chacartegui *et al*., 2016), $\boldsymbol{T_{HTT}}$	390 °C
Minimum heat transfer temperature difference (Chacartegui *et al*., 2016), $\Delta\boldsymbol{T_{min}}$	10 °C
ORC turbine efficiency (Chacartegui *et al*., 2016), $\boldsymbol{\varepsilon_{OT}}$	0.85
Generator efficiency (Li *et al*., 2019), $\boldsymbol{\varepsilon_g}$	0.95
Pump efficiency (Delgado-Torres *et al*., 2010), $\boldsymbol{\varepsilon_P}$	0.75
Internal heat exchanger efficiency (Delgado-Torres *et al*., 2010), $\boldsymbol{\varepsilon_{IHX}}$	0.8

4 RESULTS AND DISCUSSION

The thermodynamic parameters in different points are presented in Table 2. The operating temperature and pressure of SRC are similar to those in conventional dual-tank indirect CSP systems. Notably, the state points of SRC remain constant in both the rated and heat discharge modes due to the unique discharge process. The results are summarized in Table 3. The net power outputs of the SRC and ORC are 49.255 and 9.527 MW, respectively. W_{ORC} is relatively low due to the high evaporation temperature

of water (303.14ºC). The thermal efficiency of the proposed system reaches 42.01%, which is appreciably higher than that of the conventional SRC efficiency (37.93%).

Table 2: Calculated results of each state point.

State point	Temperature (°C)	Pressure (MPa)	Enthalpy (kJ/kg)	Quality (%)
1	41.51	0.008	173.84	0
2	41.60	0.875	175	subcooled
3	70.92	0.875	297.6	subcooled
4	103.86	0.875	436.02	subcooled
5	138.61	0.875	583.55	subcooled
6	172.66	0.875	730.76	subcooled
7	174.42	9	742.83	subcooled
8	212.38	9	910.9	subcooled
9	256.48	9	1117.1	subcooled
10	370	9	3026.1	superheated
11	283.52	4.54	2891.18	superheated
12	213.88	2.06	2753.88	97.61
13	213.88	2.06	2753.88	97.61
14	370	2.06	3181	superheated
15	265.37	0.875	2980.97	superheated
16	174.32	0.3627	2808.80	superheated
17	105.36	0.1224	2633.38	97.75
18	72.42	0.03461	2457.08	92.56
19	41.51	0.008	2279.26	87.64
20	46.60	0.03357	195.16	subcooled
21	75.92	0.11873	317.94	subcooled
22	108.86	0.35182	456.75	subcooled
23	179.42	1.9982	761	subcooled
24	217.38	4.4038	932.13	subcooled
25	41.51	0.008	1932.26	73.20
26sl	390	0.959	774.40	0
26	390	0.959	987.60	1
27	-	0.790	955.72	superheated
28	-	0.303	871.54	superheated
28sv	313.34	0.303	848.86	1
29	313.34	0.303	628.61	-
30	313.34	0.303	585.14	0
31	-	0.959	586.23	subcooled
32	-	0.959	670.40	subcooled

Table 3: Results of the parameters.

Parameter	Value	Parameter	Value	Parameter	Value
$\boldsymbol{m_{steam}}$ **(kg/s)**	57.489	m_{18} (kg/s)	2.118	W_{LT} (kW)	37812.85
$\boldsymbol{m_{11}}$ **(kg/s)**	6.051	m_{19} (kg/s)	36.964	W_{SRC} (kW)	49254.76
$\boldsymbol{m_{12}}$ **(kg/s)**	4.329	W_{P1} (kW)	51.44	W_{ORC} (kW)	9526.87
$\boldsymbol{m_{13} = m_{14}}$ **(kg/s)**	47.109	W_{P2} (kW)	693.70	η_{ORC}	9.20%
$\boldsymbol{m_{15}}$ **(kg/s)**	2.762	W_{P4} (kW)	335.84	m_{VP-1} (kg/s)	326.338
$\boldsymbol{m_{16}}$ **(kg/s)**	2.782	W_{OT} (kW)	10402.85	η_{SRC}	37.93%
$\boldsymbol{m_{17}}$ **(kg/s)**	2.484	W_{HT} (kW)	14818.63	$\eta_{ORC-SRC}$	42.01%

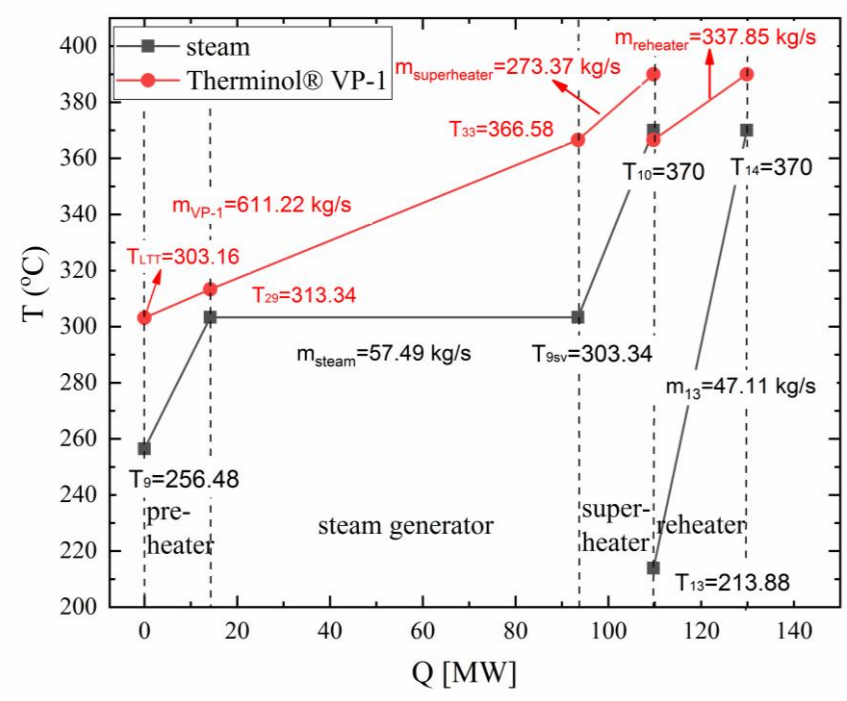

Figure 5: *T-Q* diagram in the discharge mode when T_{9sv}= 303.34 °C.

The water evaporation temperature (T_{9sv}) is a crucial parameter. T_{9sv} influences not only the cascade ORC-SRC efficiency in the normal operating conditions but also the temperature difference between the HTT and LTT. From the viewpoint of cascade cycle efficiency, the optimum T_{9sv} is expected to be lower than 303.14ºC to offer a higher ORC efficiency. The temperature difference between the oil tanks further affects power efficiency and output during the discharge mode. The *T-Q* diagrams at T_{9sv} of 303.34 °C and 260 °C are exemplified in Figs. 5 and 6 respectively. Assume the outlet oil temperatures in the superheater and reheater are the same as T_{33} in view of reduced heat transfer area. For both cases, the pinch point temperature difference (10°C) takes place when water reaches the saturated liquid state. Therminol® VP-1 is subcooled before flowing into LTT, but its temperature and enthalpy can be approximated obtained by linear interpolation in the saturated liquid parameters. m_{VP-1}, T_{33} and T_{LTT} can be calculated by the heat balance in the preheater, steam generator, superheater and reheater. T_{LTT} decreases considerably from 303.16 °C to 268.96 °C when T_{9sv} falls from 303.34 °C to 260 °C. The SRC and ORC-SRC efficiencies at T_{9sv} of 260 °C are 35.47% and 42.66%, respectively. It confirms that as the steam evaporation temperature decreases, the SRC efficiency drops but the SRC-ORC efficiency increases. The power generation capacity of the thermal oil during discharge is 103.01 kJ/kg and 80.58 kJ/kg when the LTT temperature is 268.96 °C and 303.16 °C respectively. The decrement in T_{9sv} leads to a larger thermal storage capacity.

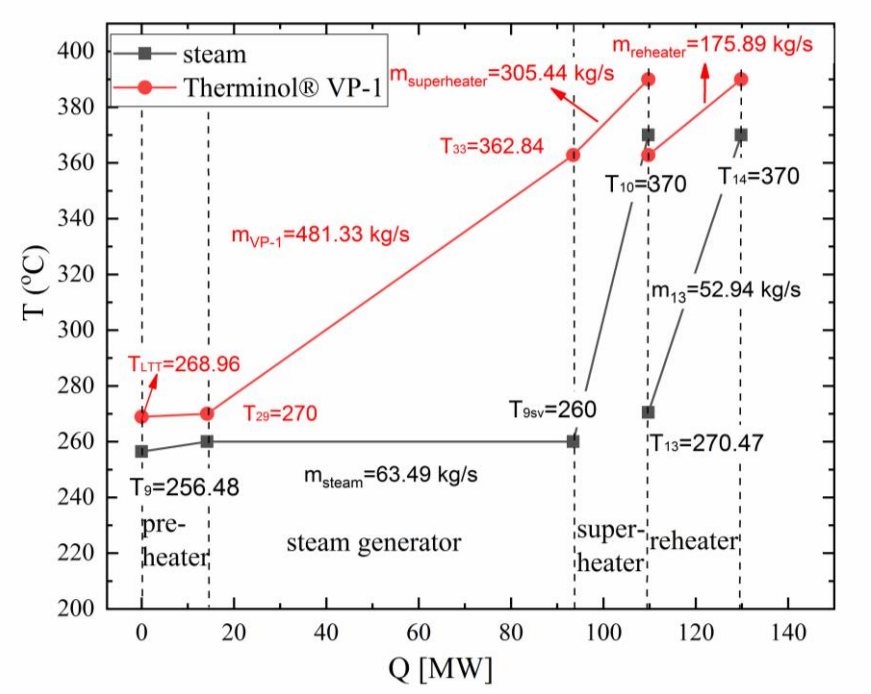

Figure 6: *T-Q* diagram in the discharge mode when T_{9sv}= 260 °C.

5 CONCLUSION

A novel direct vapor generation CSP system using cascade ORC-SRC and dual-tank structure is proposed in this paper. Therminol® VP-1 is innovatively adopted as both heat transfer and storage medium, as well as ORC fluid. Compared with the conventional dual-tank CSP systems using thermal oil as the heat transfer medium, the collectors benefit from efficient heat transfer in the binary region of Therminol® VP-1 and a high solar field efficiency can be achieved. Besides, the drawbacks of small heat storage capacity and part-load operation of the power block attributed to the limited temperature drop in the single-tank systems are eliminated. Both the rated and heat discharge modes are elaborated. The results indicate that the thermal efficiency of the novel system is significantly higher, and the increment is from 37.93% to 42.01%.

NOMENCLATURE

CF	closed feedwater		P	pressure	(MPa)
CSP	concentrated solar power		P	pump	
EHST	equivalent hot side temperature (K)		PCM	phase change material	
h	specific enthalpy	(kJ/kg)	s	specific entropy	(kJ/kg/K)
HTT	high temperature tank		SRC	steam Rankine cycle	
I	irradiance	(W/m^2)	T	temperature	(°C)
IHX	Internal heat exchanger		v	specific volume	(m^3/kg)
LTT	low temperature tank		W	work	(kW)
m	mass flow rate	(kg/s)	x	extraction percentage	(%)
OF	open feedwater		ε	device efficiency	(%)
ORC	organic Rankine cycle		η	efficiency	(%)

Subscript

1 ... 32	number	LT	low-pressure turbine
b	basic	min	minimum
DN	direct normal	s	isentropic
g	generator	$steam$	steam
HT	high-pressure turbine	sv	saturated vapor

sl	saturated liquid	$VP-1$	Therminol® VP-1 cycle

REFERENCES

Boukelia, T.E., Arslan, O., Mecibah, M.S., 2016, ANN-based optimization of a parabolic trough solar thermal power plant, *Applied Thermal Engineering*, vol. 107, p. 1210-1218.

Casati, E., Galli, A., Colonna,P., 2013, Thermal energy storage for solar-powered organic Rankine cycle engines, *Solar Energy*, vol. 96, pp. 205-219.

Chacartegui, R., Vigna, L., Becerra, J.A., Verda, V., 2016, Analysis of two heat storage integrations for an Organic Rankine Cycle Parabolic trough solar power plant, *Energy Conversion and Management*, vol.125, p. 353-367.

Concentrating Solar Power Projects by Technology-NREL. https://solarpaces.nrel.gov/by-technology (accesed 7 July 2021)

Delgado-Torres, A.M., García-Rodríguez L., 2010, Analysis and optimization of the low-temperature solar organic Rankine cycle (ORC), *Energy Conversion and Management*, vol. 51, p. 2846-2856.

Eastman Corp https://www.eastman.com/Literature_Center/T/TF9141.pdf (accesed 3 July 2021)

Li, J., Gao, G.T., Kutlu C., Liu K., Pei, G., Su, Y.H., Ji, J., 2019, A novel approach to thermal storage of direct steam generation solar power systems through two-step heat discharge, *Applied Energy*, vol. 236, p. 81-100.

Li, J., Alvi, J.Z., Pei, G., Ji, J., Li, P.C., Fu, H.D., 2016, Effect of working fluids on the performance of a novel direct vapor generation solar organic Rankine cycle system, *Applied Thermal Engineering* vol. 98, p. 786-797.

Li, J., Jahan, Z.A., Pei, G., Su, Y.H., Li, P.C., Gao, G.T., Ji, J., 2016, Modelling of organic Rankine cycle efficiency with respect to the equivalent hot side temperature, *Energy*, vol. 115, p. 668-683.

Mohammadi, K., McGowan, J. G., 2018, Thermodynamic analysis of hybrid cycles based on a regenerative steam Rankine cycle for cogeneration and trigeneration, *Energy Conversion and Management*, vol. 158, p. 460-475.

Montes, M.J., Abánades, A., Martínez-Val, M.J., Valdés, M., 2009, Solar multiple optimization for a solar-only thermal power plant, using oil as heat transfer fluid in the parabolic trough collectors, *Solar Energy*, vol. 83, p. 2165-2176.

Padilla, R.V., 2011, Simplified Methodology for Designing Parabolic Trough Solar Power Plants, University of South Florida, *Graduate School Theses and Dissertations*.

Vescovo, R., 2019, High temperature organic Rankine cycle (HT-ORC) for cogeneration of steam and power. *AIP Conference Proceedings* 2191, 020153.

ACKNOWLEDGEMENT

The study was sponsored by the Anhui Provincial Natural Science Foundation (2008085QE235), Fundamental Research Funds for the Central Universities of China (JZ2020HGTA0074), DONGFANG ELECTRIC Dongfang Boiler Group CO., LTD.